PALEOBIOLOGY
A PUBLICATION OF THE
Paleontological
S O C I E T Y

Restricted morphospace occupancy of early Cambrian reef-building archaeocyaths

David R. Cordie and *Stephen Q. Dornbos*

Abstract.—The evolution of novel morphologies can signify expansion of a clade into new niches. This can be studied in the fossil record by investigating the morphospace occupancy of organisms, with small morphospaces signifying low morphological disparity and more diffuse morphospaces suggesting a broader range of morphologies adapted to different environments. Morphological disparity of many taxa (arthropods, crinoids, etc.) from the Cambrian to modern intervals have been studied in this manner. However, no study has investigated this in archaeocyaths, which, as reef builders, can have a disproportionate effect on early Cambrian biodiversity relative to their frequency. Here, we collect morphological data on archaeocyathan sponges, mostly from Laurentia. More than 600 museum specimens and 400 field samples were measured for traditional morphometric characters and discrete gross morphological characteristics. We find that archaeocyaths have an average cup/individual (body) diameter of 10.6 mm. This is significantly smaller than a selected group of modern demosponges and lithistid sponges that measure 94.1 mm and 66.8 mm in diameter, respectively, and each has a larger size variance. Archaeocyathan gross morphologies are also highly constrained to a few simple morphologies (three to six categories), while modern demosponges and lithistids are more diverse (nine categories each). These data indicate that Laurentian archaeocyaths were restricted in their morphological disparity, potentially due to limitations imposed by having a robust calcareous skeleton while still maintaining a large intervallum cavity space to facilitate passive entrainment. The fact that these Cambrian reef builders were restricted in their morphological complexity may have had a strong influence on the biodiversity of early Phanerozoic ecosystems. Furthermore, a clade limited to only a few specific morphologies is at an increased risk of extinction.

*David R. Cordie and Stephen Q. Dornbos. Department of Geosciences, University of Wisconsin–Milwaukee,
Milwaukee, Wisconsin 53201, U.S.A. E-mail: drcordie@uwm.edu, sdornbos@uwm.edu*

Introduction

The survival of any clade is dependent on the ability of taxa included within it to gather resources necessary for survival. Previous studies on crinoids (Kammer et al. 1997, 1998), gastropods (Gili and Marinell 1994), bivalves (Stanley 1986; Jablonski and Hunt 2006), modern fish (Wilson et al. 2007), and carnivores (Gray et al. 2016) have shown that a more generalist lifestyle can promote greater taxon longevity (Raia et al. 2016). Therefore, it is prudent for taxa to expand into new niches to take advantage of multiple resources, and often this requires the adaptation of novel or expanded morphological features (Hellberg et al. 2001; McCormack and Smith 2008; Bellwood et al. 2014). This can be observed in the fossil record as taxa expanding their distribution within morphospace due to an adaptive radiation, often when presented with sufficient ecological opportunity (Losos 2010). Morphospace is the mathematical and/or graphical depiction of the morphology of an organism and can be used as a proxy for exploring the occupancy of niches by extinct organisms (Mitteroecker and Huttegger 2009).

Organisms tend to occupy far less morphospace than what is theoretically available (Raup 1966). However, the distribution and location of taxa within morphospace can be informative of the evolutionary history and paleoecology of an organism (Ritterbush and Bottjer 2012; Huang et al. 2014). For example, morphospace studies of Cambrian organisms have suggested that disparity was similar to modern organisms (Briggs et al. 1992), but may have shifted through time (Willis 1998; Löfgren et al. 2003). Furthermore, this pattern of early maximum disparity may have also occurred before the Cambrian radiation during the Ediacaran (Shen et al. 2008). However, these

trends are not consistent across all groups of organisms, with blastoids (Foote 1992), stylophorans (Lefebvre et al. 2006), and onychophorans (Yang et al. 2015) as notable exceptions. This body of research is often framed as determining whether organisms reached an early maximum of morphological disparity, and subsequent decimation, or disparity was proportional to taxonomic diversity (Gould 1991; Erwin 2007). Here, we investigate the morphological disparity within a different group of taxa, archaeocyathan sponges, to quantify the morphospace occupancy of a common early Cambrian reef builder.

Previous Work

Research on the morphology of sponges can be challenging due to the lack of easily definable characters (i.e., landmarks) and the plastic nature of their modular morphology. For instance, sponges are known to increase spicule density and constrict their central cavity in high-energy environments (Palumbi 1984, 1986). Gross morphology of sponges is also influenced by environment, with more fragile branching forms common in lower-energy environments (Bell and Barnes 2000; Bell et al. 2002). But, looking at the fossil record of ancient sponges and their morphological disparity can inform us of the variety of environments in which those organisms existed. Archaeocyathan morphological disparity is particularly important, because archaeocyaths were framework builders, which could have disproportionally affected their surroundings and local biodiversity (Erwin 2008; also see Watkins [2000] and Hageman and McKinney [2010] for morphological studies on other reef builders). A more restricted or expanded morphological disparity can give us more information about the filling of ecospace during the early (Terreneuvian–Series 2) Cambrian.

Archaeocyaths are preserved as three-dimensional calcitic cups within a rock matrix. Cut or naturally weathered faces expose a two-dimensional cross section of the cup within the matrix. Archaeocyaths within the order Monocyathida have a single wall; however, the vast majority of archaeocyaths have a unique double-walled structure separated by an open cavity, the intervallum. During life, the intervallum was potentially the location of the bulk of soft tissue, but postmortem this cavity appears open. The two walls may be connected by up to several hundred radial-longitudinal septa and transverse tabulae, though either feature may be absent. Where they present, these skeletal elements together form chambers known as loculi. The inner wall encloses a central cavity with a distal osculum. Prior research on archaeocyaths has used a functional morphology approach to show that pore (ostia) density is important in creating strong water channelization and flow direction, much as in other poriferans (Balsam and Vogel 1973; Savarese 1992). Additional morphological studies of archaeocyaths related the central cavity size to their paleoenvironments (Savarese 1995) and categorized their cup integration (Wood et al. 1992). However, little work on archaeocyathan morphology has been performed since, and no extensive studies of archaeocyathan morphology from museum collections have been performed to date. Therefore, we collected measurements from several museum collections and discrete gross morphological characters from databases to amass a large (>1000 specimens) data set of archaeocyathan morphology. We find that archaeocyaths, the primary metazoan reef builders of the early Cambrian, were restricted in their morphological disparity and, therefore, in the paleoenvironments they inhabited.

Materials and Methods

Archaeocyaths are, often, the most common metazoan framework builder in early Cambrian reefs. Additional enigmatic metazoans also occur in some localities. For example, coralomorphs (Hicks 2006), radiocyaths (Kruse et al. 1996), or other sparse calcareous sponges do occur (Reitner et al. 2017). However, we focus here on archaeocyaths, as few specimens of these other reef builders were available and were comparatively minor in diversity.

Two comparative data sets were assembled to assess the differences between archaeocyathan morphology and other reef-building organisms, the modern demosponges and lithistid sponges. First, modern demosponges contain several examples of calcareous

organisms, for example, *Vaceletia* and *Calcifibrospongia*, as well as several orders with aspiculate micromorphology, for example, Dictyoceratida, Verongiida, and Dendroceratida, which instead are composed of spongin fibers. Taxonomically, archaeocyaths are suggested to either be closely related to or members of Demospongiae (Debrenne and Zhuravlev 1994; Rowland 2001). However, demosponges occur in more environments than archaeocyaths, for example, deep marine, which allows for greater innovation of novel morphologies. Thus, a second data set consisting of polyphyletic lithistid demosponges sponges was also assembled. Samples used in this study ranged in age from the Paleozoic ($N = 42$), Mesozoic ($N = 8$), Paleogene ($N = 5$), to modern ($N = 38$). Lithistid sponges form robust calcifying reefs in both ancient and modern ecosystems. They possess spicules called desmas and typically inhabit tropical to temperate environments alongside demosponges (Schuster et al. 2015). Therefore, we include data on modern demosponges (here referring to extant non-lithistid varieties), as they are a single taxonomic group that may include Archaeocyatha, and a second data set of lithistid sponges (here referring to fossil and modern heavily calcified demosponges within the polyphyletic group "Lithistida"), as they are the closet ecologically analogous organism to archaeocyaths. Two separate methods of analysis were used as part of this study, one using continuous variables and a second with discrete variables.

Continuous variables for archaeocyaths were measured on cross sections preserved in rock slabs ($N = 1108$) from museum collections at the University of California Museum of Paleontology (UCMP), the University of Alaska Museum of the North (UAMES), and the University of Wisconsin–Milwaukee (IESAG) and field samples from the Poleta and Harkless Formations near Lida, Nevada, USA. Museum-based specimens ($N = 630$) are the primary focus of all analysis except when indicated otherwise and contain samples from three paleocontinents: Laurentia, Gondwana (Australia), and Mongolia (Zhavkhan Terrane) (Fig. 1A). Our data set is heavily biased toward samples from Laurentia (>82%), thus the trends

discussed below may be more indicative of archaeocyaths from Laurentia, rather than a global phenomenon. Regardless, our data still represent a major paleocontinent with substantial biodiversity.

Measurements of cup/individual diameter (hereafter referred to as body size), osculum diameter (hereafter referred to as osculum size), loculus width, and septal thickness were collected for all museum specimens (Fig. 1B). Only body- and osculum-size measurements were collected for field samples. For all body- and osculum-size measurements, two diameters were measured, one at the point of maximum width and a second perpendicular to the first measurement (Fig. 1B). These two values were averaged to reduce bias due to oblique cross sections. Samples that appeared to be extremely obliquely crosscut or fragmented were excluded. Personal observations of three-dimensionally preserved archaeocyaths suggest that they are not always perfectly circular in cross section, but rather more elliptical. Therefore, we prefer this two-diameter method to simply using either minimum or maximum diameters to characterize body size. Multiple loculus width measurements (average 1.9 per specimen) were collected from the inner wall side when available and averaged. Loculus measurements were taken at various positions around the cup to capture variability of width. Septal thickness was measured at the midpoint between the inner and outer wall. Intervallum area percentage was determined by using equation (1).

$$I\% = \left[\left(\text{area of body} - \text{area of osculum} \right) / \text{area of body} \right] \times 100 \qquad (1)$$

Data from modern demosponges ($N = 71$) were collected on museum specimens housed at the Milwaukee Public Museum (MPM) for body size, osculum size, and maximum height following the method used for the archaeocyath data set. Measurements were made using a digital caliper accurate to within 0.01 mm. Lithistid sponge data were collected from the primary literature either from dimensions specified in the text or directly from figures ($N = 93$; see Supplementary Materials for reference
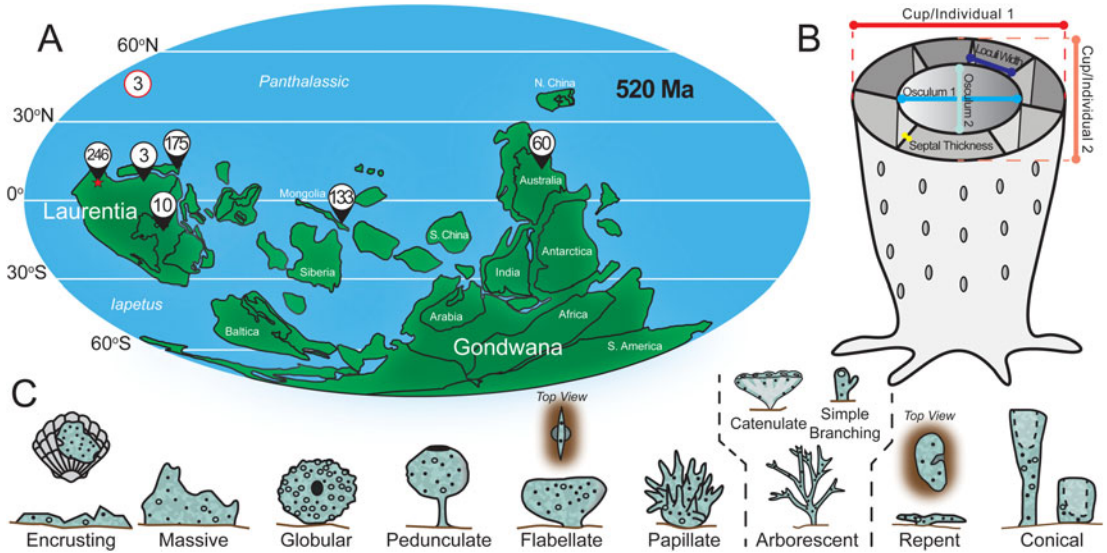
FIGURE 1. Overview of materials and methods. A, Paleogeography of early Cambrian with locality information of museum samples measured for continuous variables ($N = 630$). Upper left-hand value denotes unknown locality. Field sample locality denoted by star. B, Diagram of archaeocyath annotated with measurements taken for continuous variables. C, Nine morphological categories used in discrete character analysis (based on Bell and Barnes 2001). Arborescent category includes catenulate and simple branching morphologies. See Boury-Esnault and Rützler (1997) for definitions of categories and Supplementary Material for synonymized categories.

list). Both modern and fossil examples of lithistid sponges were included.

Discrete morphological variables were compiled from database entries. Archaeocyathan gross morphology, cup shape, and elaboration (ridges, spines, troughs, etc.) for all valid genera of archaeocyaths ($N = 309$) were gathered from the online database Archaeocyatha—A knowledge base (Kerner et al. 2011). For comparison, all extant, marine taxa of 'Demospongiae Sollas, 1885', using the 'only accepted names' and 'all records' filters, were compiled from the World Porifera Database ($N = 6274$). Using a random number generator, a random subset of 300 taxa were selected from this list and assessed for gross morphology based on their descriptions in *Systema Porifera* (Hooper and Van Soest 2002). Lithistid sponge gross morphology was assessed from the same literature survey as the continuous variables. For all data, binary presence or absence coding was performed to determine the percentage of organisms that can display each morphological category as seen in Bell and Barnes (2001: Fig. 2; Fig. 1C in the present study).

Within the continuous data set, a permutational multivariate analysis of variance (PERMANOVA; 10,000 replicates, Mahalanobis distance) analysis of archaeocyath measurements was performed across locality, taxonomic order, and geologic formation groups. Mann-Whitney U and Levene's tests were performed on logarithmically transformed body size and osculum size for archaeocyaths versus modern demosponges and lithistid sponges to determine differences in size and variance. To quantify the magnitude of difference between our test groups, we used Cohen's d to calculate effect size of two independent means based on equation (2).

$$d = (\text{mean of group A} - \text{mean of group B})/ \text{SD}_{\text{pooled}}$$

(2)

In our analysis, an effect size larger than 0.80 is considered large (Cohen 1992). Coupled with hypothesis testing, Cohen's d provides information not just about the occurrence of a statistical difference, but also about the size of the difference in means. For the discrete data set, a χ^2 test was performed on archaeocyathan versus modern demosponge and lithistid sponge
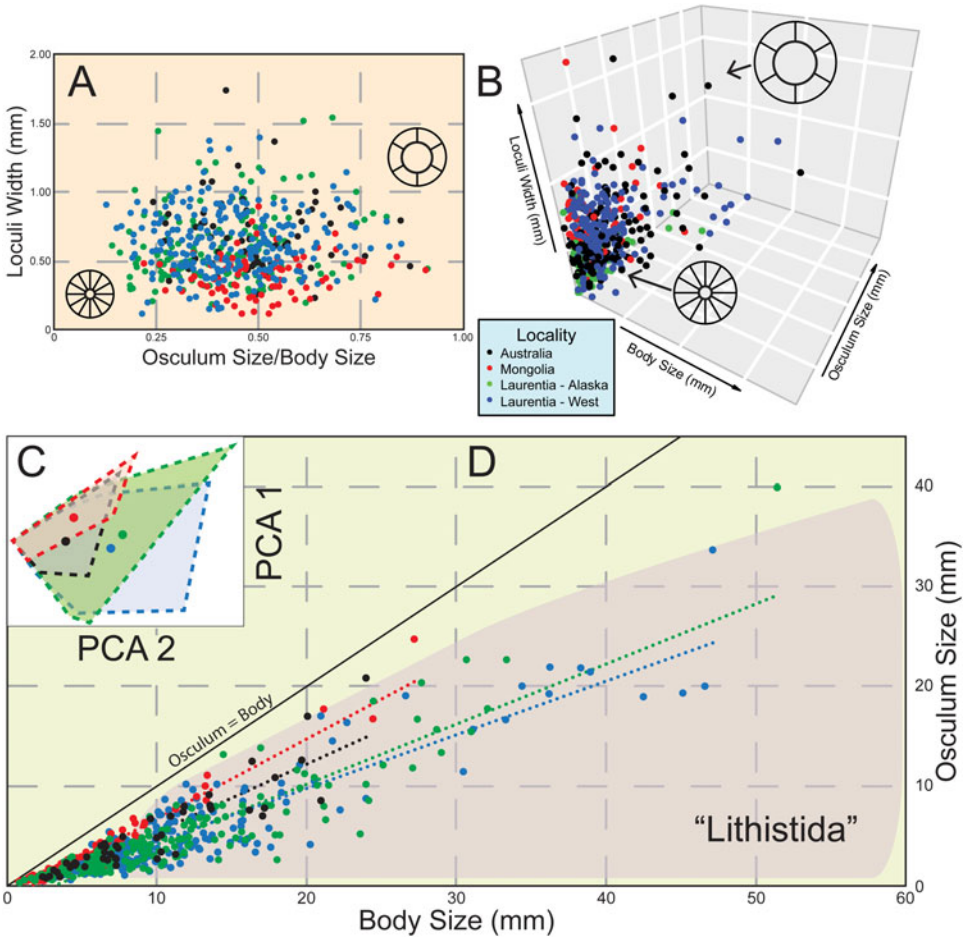
FIGURE 2. Continuous variable measurements for museum specimens of archaeocyaths. A, Two-dimensional morphospace with colors showing general locality. Color scheme same throughout figure. Readers are directed to the online version of this article for color figures. B, Three-dimensional morphospace with colors showing general locality. C, Principal component analysis of five continuous variables. Convex hulls with centroid centers shown. First axis accounts for 96.3% of variance. D, Body- and osculum-size relationship with linear trend lines for locality. Approximate morphospace distribution of lithistid sponges shown in shaded region. $N = 544$ for A and B; $N = 630$ for C and D. Raw data available in the Supplementary Material.

gross morphologies. All statistical tests were performed in Past v. 3.14.

Results

Archaeocyathan Morphology

Archaeocyathan body size averaged 10.6 mm and had a right skew with a maximum diameter of 74.0 mm. Osculum size averaged 5.0 mm and had a right skew with a maximum size of 59.5 mm. Loculus width averaged 0.60 mm and septal thickness averaged 0.24 mm. Archaeocyathan cross sections were on average

21.8% intervallum compared with osculum area (Table 1). Nearly all samples were two-dimensional cross sections that did not allow for height measurements, but one three-dimensionally preserved specimen had a height of 22.9 mm, and a second fragmented sample measured more than 110 mm.

In both two-dimensional and three-dimensional morphospace, archaeocyaths tend to cluster near smaller body, osculum, and loculus sizes (Fig. 2A,B). Archaeocyaths from Mongolia appear to have narrower loculi compared with all other localities. However,

TABLE 1. Size measurements (mm) for all archaeocyaths (museum and field), lithistid sponges, and modern demosponges. The 95% confidence intervals are given in parentheses. *Based on one specimen (UCMP 220889).

Taxa	Body average	Body minimum/ maximum	Osculum average	Osculum minimum/ maximum
Archaeocyatha	10.6 (10.1–11.0)	0.8–74.0	5.0 (4.7–5.3)	0.3–59.5
"Lithistida"	66.8 (53.8–79.8)	5.0–400.0	—	—
Modern Demospongiae	94.1 (72.9–119.7)	9.1–490.0	17.8 (12.4–23.3)	1.2–53.5

Taxa	Loculus width average	Septal thickness average	Intervallum area %	Maximum height average
Archaeocyatha	0.60 (0.58–0.62)	0.24 (0.22–0.24)	21.8 (20.7–22.9)	22.9*
"Lithistida"	—	—	—	75.7 (59.7–93.7)
Modern Demospongiae	—	—	—	188.4 (138.0–193.8)

principal component analysis (PCA) shows there is a substantial amount of overlap (Fig. 2C). Different taxonomic orders do have significantly different body sizes, with the largest being Capsulocyathida (28.8 mm, $N = 7$), followed by Ajacicyathida (12.8 mm, $N = 240$), and Archaeocyathida (11.5 mm, $N = 383$). However, taxonomic groups also appear to have large amounts of morphospace overlap (Supplementary Fig. 1). Osculum size is highly correlated with body size ($r = 0.91$). Osculum sizes from localities within Laurentia appear to be more similar to one another than to those of specimens from more distant localities (Fig. 2D). Continuous variables measurements failed multivariable tests of normality, therefore, nonparametric permutation tests were required. Archaeocyaths did display differences in centroid means based on locality (PERMANOVA p-value < 0.001), taxonomic order (PERMANOVA p-value < 0.001), and geologic formation (PERMANOVA p-value < 0.001). See Supplementary Figs.1 and 2 and Supplementary Tables 1–3 for pairwise comparisons.

Contrasting Archaeocyaths to Other Sponges

Continuous Variables.—Modern demosponge body sizes measured in this study average 94.1 mm and have a substantially higher maximum value of 490.0 mm, while osculum size averaged 17.8 mm and a maximum value of 53.5 mm. Average height of these organisms is 188.4 mm (Table 1). Some modern demosponges are entirely within the range of archaeocyathan body size (e.g., *Dactylia*, *Spongia*, and *Fasciospongia*), and minimal sizes for many others are also within this range (Fig. 3A). However, the average sizes for most demosponges and nearly all maximum values are above the maximum size for archaeocyaths. Approximately 45% of modern demosponges are larger than the largest archaeocyath (Fig. 3B). On the other hand, osculum sizes are more similar (Fig. 3A). Modern demosponge body size is significantly different (Cohen's $d = 2.4$, Mann-Whitney U p-value < 0.001) from archaeocyathan body size. Osculum size is also significantly different (Cohen's $d = 1.4$, Mann-Whitney U p-value < 0.001). Variance between body size (Levene's p-value < 0.001), but not osculum size (Levene's p-value = 0.53), is also significantly different.

Lithistid sponge body size averaged 66.8 mm with a maximum value of 400.0 mm. Average height of these organisms was 75.7 mm. Similar to modern demosponges, minimum body size was within the range of variability of archaeocyaths, but 94.6% of lithistid sponges were larger than the average archaeocyath, and 26.8% were larger than the largest archaeocyath. Both body size (Cohen's $d = 2.3$, Mann-Whitney U p-value << 0.001) and body variance (Levene's p-value = 0.022) were significantly different between archaeocyaths and lithistid sponges.

As a check on our methodology, all comparisons were repeated using only minimum diameter measurements for body size and
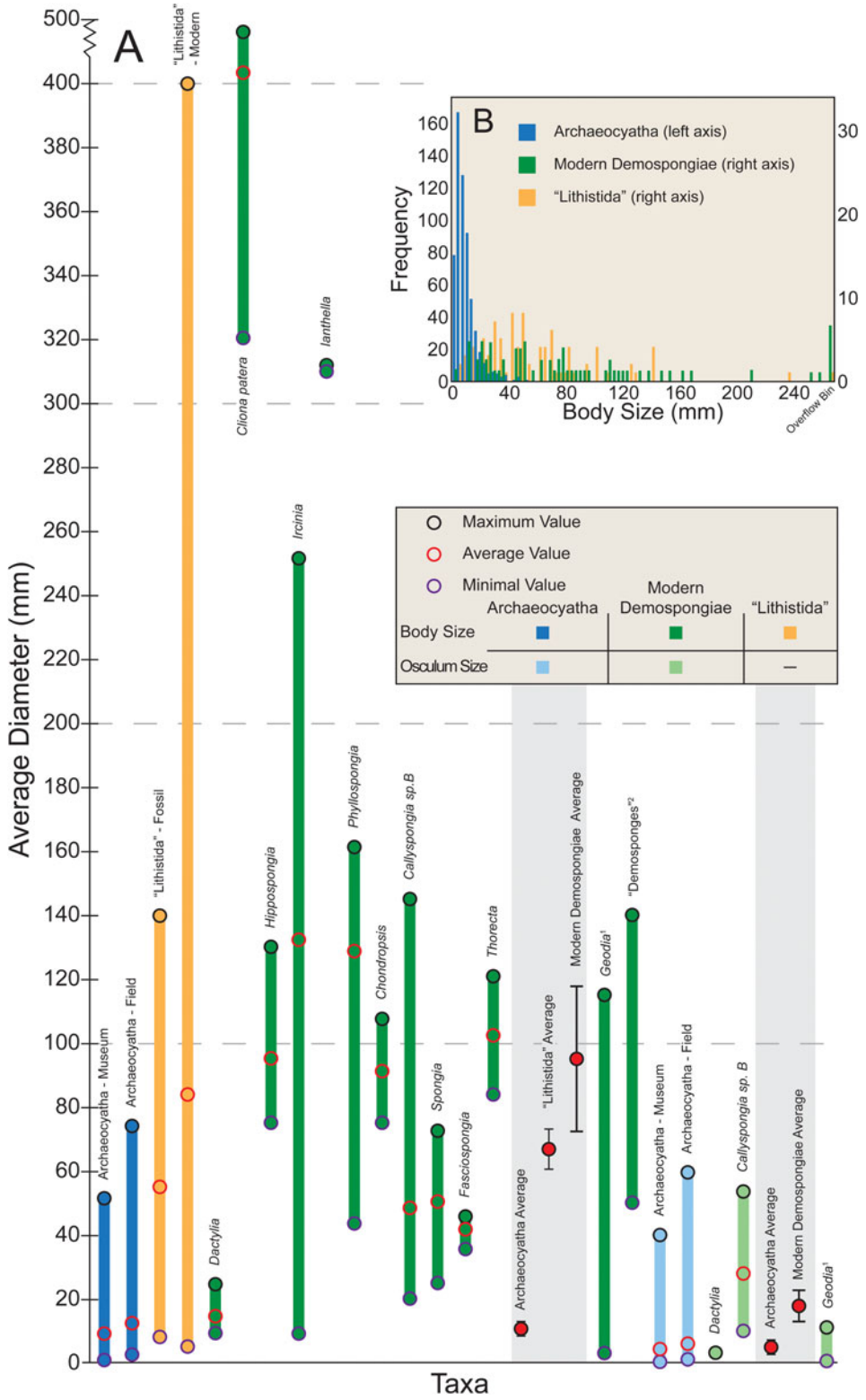
osculum sizes. All comparisons of mean body and osculum sizes using Mann-Whitney U-tests show significantly smaller sizes of archaeocyathan minimum diameters in comparison to either modern demosponges or lithistid sponges. Variances in minimum body and osculum sizes were also significantly smaller in archaeocyaths compared with either group based on Levene's test. In summation, all results presented above were reproduced using only minimum diameters with the exception of osculum variance, which was found to be significantly smaller in archaeocyaths compared with modern demosponges at $\alpha = 0.05$, but not at $\alpha = 0.01$ (see Supplementary Table 4).

Discrete Variables.—Our random sampling of demosponge gross morphologies has a similar distribution to those observed directly in field studies, with the most common morphology being encrusting (Fig. 4A). By comparison, most archaeocyaths display simple branching morphology. Lithistid sponges, on the other hand, most commonly display a conical or globular gross morphology, but still occupy many of the other categories in comparison with archaeocyaths. The distribution of morphologies between archaeocyaths and either modern demosponges or lithistids is significantly different (effect size = 0.7 and 1.4, respectively, χ^2 p-value < 0.001 for both comparisons). Furthermore, archaeocyaths are extremely uniform beyond gross morphology, as 95% have simple cylindrical-conical cup shapes (Fig. 4B) and 92% have no external elaboration (Fig. 4C).

Discussion

Morphological Disparity within Archaeocyatha

Archaeocyaths displayed a narrow range of continuous character variation, but there were differences between localities (Fig. 2). For example, archaeocyaths from Laurentia tend to have larger loculi and smaller oscula compared with archaeocyaths from Mongolia

(Fig. 5A–E). Archaeocyaths from different parts of Laurentia were more similar to one another than to archaeocyaths from more distant locations, especially in terms of osculum size (Fig. 2C,D). PCA plots also show similar results, with the center of convex hulls shifted right for Laurentian archaeocyaths compared with archaeocyaths from Mongolia and Australia (Fig. 2C). PERMANOVA results support these visual assessments by finding significant differences in centroid means across the different localities. However, it would be difficult to assign a specific morphotype to any particular locality. There is a large amount of overlap in occupied morphospace in both two-dimensional and ordination-based morphospaces (Fig. 2A,C). Archaeocyaths with small body sizes appear to be restricted in the amount of variability they possess. Small organisms can only have small oscula and loculi as a result. Therefore, smaller archaeocyaths converge on one section of morphospace. It is possible that only larger, and most likely older, organisms had adapted to local environmental conditions. Even with larger specimens, there is no definitive separation between morphospace occupancy of different localities.

Statistical testing of archaeocyath continuous variables also found differences in centroid means based on taxonomic order and geologic formation groups (Supplementary Tables 2–3). However, as for differences based on locality, three-dimensional morphospace plots show no definitive pattern or separation of morphospace occupation based on taxonomic order or geologic formation (Supplementary Figs. 1, 2). This reaffirms our interpretation that archaeocyaths display a narrow range of morphospace occupancy based on continuous characters.

Discrete character analysis also showed very little diversity across archaeocyaths. Of 309 archaeocyath genera, 257 (83.2%) display the most common type of overall morphology (cylindrical-conical cup shape, no elaboration, arborescent gross morphology). This pattern

---

FIGURE 3. Size comparison of archaeocyaths, lithistid sponges, and modern demosponges. A, Range and average diameter sizes for archaeocyaths, lithistid sponges, and modern demosponges. Note break in y-axis. $N = 1108$ for Archaeocyatha average; $N = 93$ for "Lithistida" average; $N = 71$ for modern Demospongiae average. Error bars on averages represent 95% confidence intervals. See Supplementary Material for specimens and measurements. Readers are directed to the online version of this article for color figures. Notes: 1, Barthel and Brandt 1995; 2, Ghiold et al. 1994. B, Histogram of sponge body sizes. Right side truncated. Raw data available in the Supplementary Material.
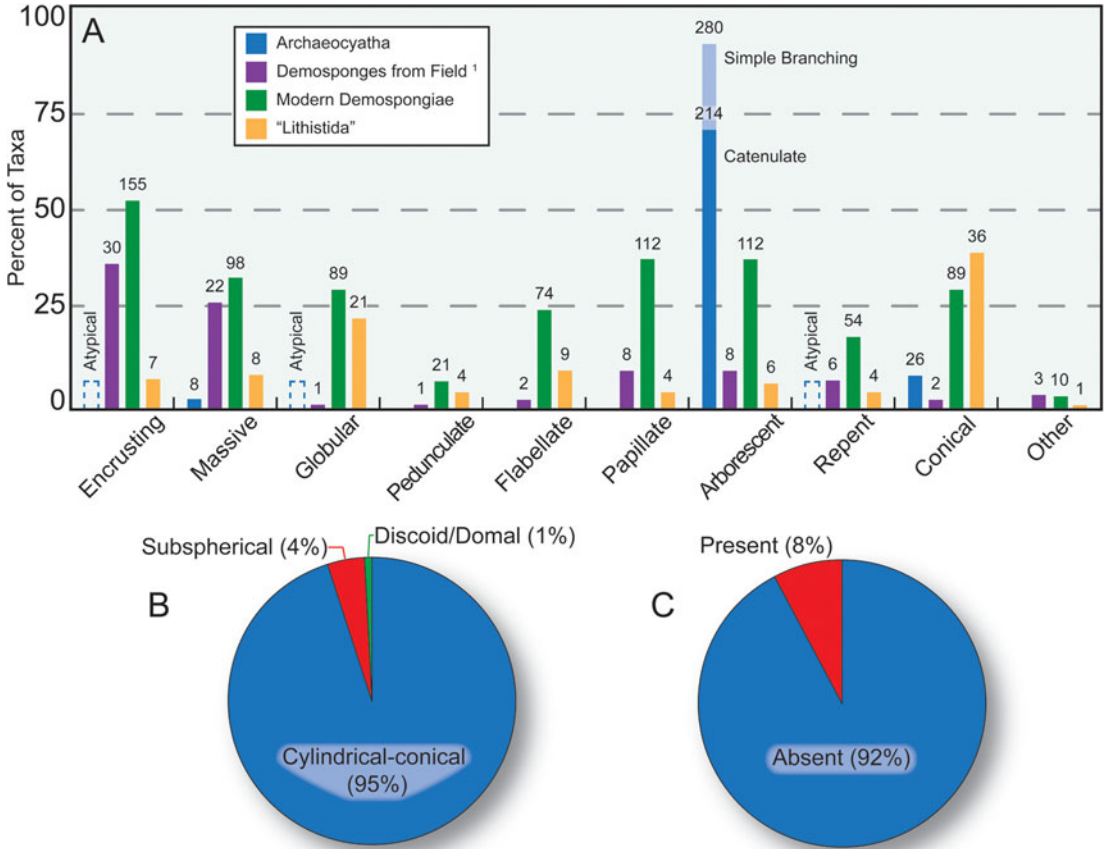
FIGURE 4. Discrete character distribution for archaeocyaths, lithistid sponges, and modern demosponges. A, Percent of taxa that display each morphological category. Some species display more than one morphology, hence values will not add to 100%. Numbers above bars indicate absolute number of taxa in each category, while height of bars indicates percentage. Atypical archaeocyath gross morphology shown in dashed boxes. Readers are directed to the online version of this article for color figures. Note1, Demosponges from field measured in Bell and Barnes (2001). B, Circle graph of archaeocyath cup shape. C, Circle graph of archaeocyath elaboration. Raw data available in the Supplementary Material.

was consistent through time and across different paleocontinents (Supplementary Figs. 3, 4). Based on descriptions used in the Archaeocyatha database, archaeocyaths only occupy three of our gross morphological categories. However, this might be an underestimate of their morphological disparity. Atypical archaeocyaths, such as *Retilamina*, *Fransuasaecyathus*, *Erismacoscinus*, and *Zunyicyathus*, can have an encrusting, globular, repent or stromatoporoid-grade gross morphology (Savarese and Signor 1989; Debrenne et al. 1990, 1991; Debrenne and Zhuravlev 1992). These additional forms bring the total to six gross morphological categories. However, these forms are limited in both generic richness and abundance.

Nonetheless, we reanalyzed our data with atypical morphologies included, by assuming an arbitrarily high proportion of genera belonged to these atypical categories (20%), and still found the proportion of differences between morphological categories to be statistically different (χ^2 p-value < 0.001).

The lack of morphological disparity within archaeocyaths, for both discrete and continuous variables, suggests minimal morphological distinctiveness within early Cambrian reef-building sponges. In fact, their limited morphology limits their realized niche space to patchy hard substrates or cryptic environments, reducing their utility as reef builders and ecosystem engineers (see Wood 1995). We do not suggest
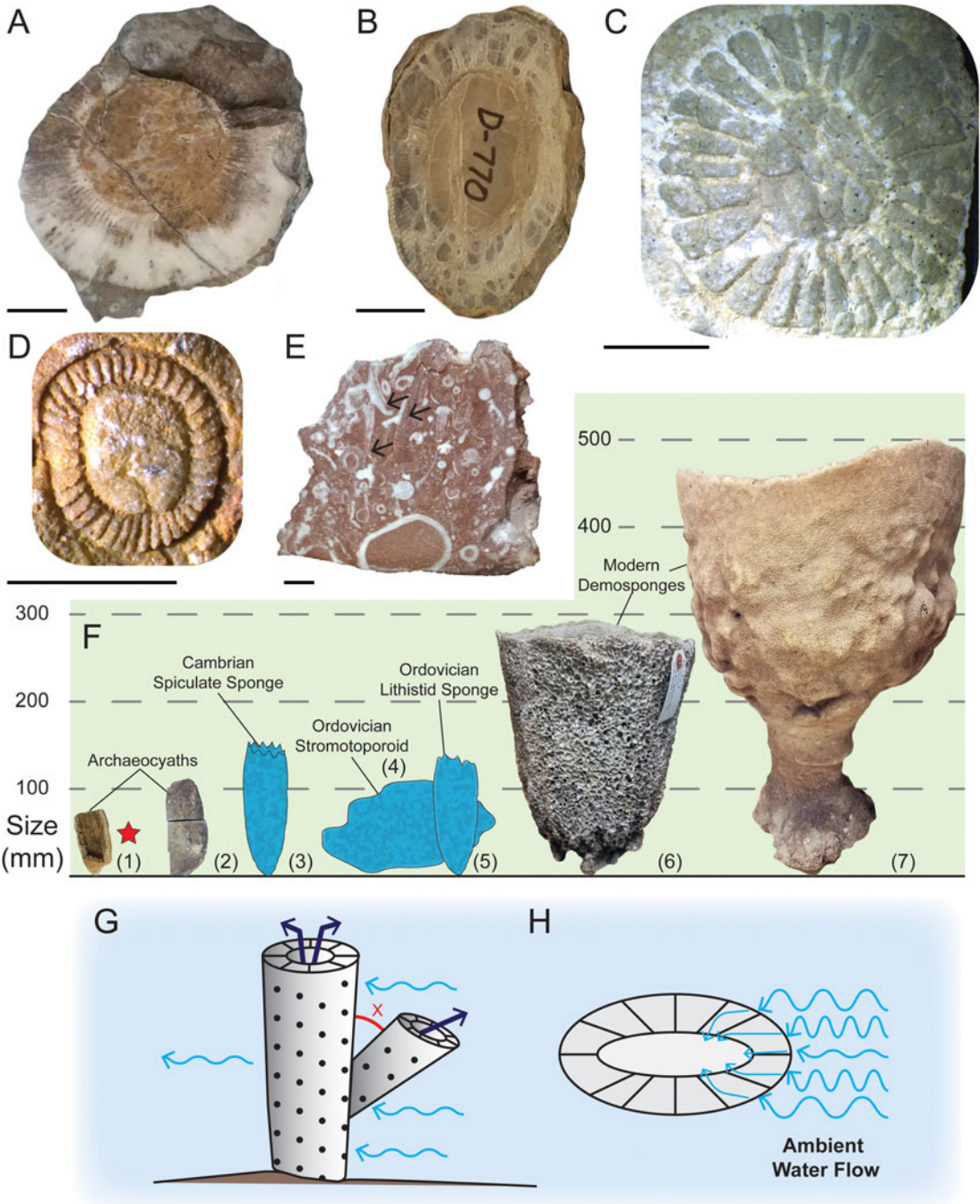
FIGURE 5. Archaeocyaths and modern demosponges used in study. A, Archaeocyath from western United States, UCMP 220846. B, Archaeocyath from western United States, UCMP 220710. C, Archaeocyath from Alaska, USA, UAMES 6099. D, Archaeocyath from Australia, UAMES 42655. E, Archaeocyath from Mongolia, IESAG000R. *Okulitchicyathus* fragments labeled with arrows. F, Size comparison of various sponges. Notes: 1, Archaeocyatha, UCMP 220822; 2, Archaeocyatha, UCMP 220858; 3, *Lantianospongia* (Xiao et al. 2005); 4, *Stratodictyon* (Webby 1979); 5, *Zittelella* (Liu et al. 2003); 6, *Ircinia*, MPM 44; 7, *Cliona patera*, MPM 53. Starred specimen is vertically exaggerated. G, Archaeocyath capturing ambient current. Angle (x) must be large enough to allow flow to reach main cup. H, Cross section of archaeocyath cup with septa redirecting and channelizing current into central cavity. Scale bars, 10 mm (A, B); 5 mm (C–E).

that archaeocyaths were completely excluded from other environments, only that they had a limited ability to thrive in many environmental settings.

It should be noted that the gross morphological characters are only a small portion of those used for taxonomic classification within Archaeocyatha. Cup diameter, osculum diameter, septal thickness, and loculus width are not taxonomically significant above the species level. Characters such as wall type, pore shape, and distribution, as well as other microscopic features (bracts, canals, microporous sheaths, etc.), would also need to be considered for classification purposes. Therefore, we do not intend here to comment on the taxonomic diversity within archaeocyaths based on these traits at this time.

Comparisons between Archaeocyaths and Other Sponges

Archaeocyaths occupy fewer regions of morphospace (Fig. 2D), have a lower range of morphological variation (Table 1), and are found to be smaller on average compared with either modern demosponges or lithistid sponges (Fig. 3A,B). Specifically, the maximum size of archaeocyaths in this study was often smaller than the minimum size of modern demosponges. The largest documented archaeocyaths belong to the plate-like genus *Okulitchicyathus*, which has possible examples of 1.5 m diameter cups (Hill 1964). However, this perceived diameter could be due to multiple layered specimens, and more conservative estimates suggest a maximum diameter of 500 mm (Debrenne et al. 2015). Even these conservative estimates most likely represent outliers for archaeocyathan body size (Fig. 5E). Regardless, this is considerably smaller than the largest species of modern demosponges such as *Xestospongia muta* (barrel sponges), which can measure 0.98 m in diameter (McMurray et al. 2008), not to mention even larger hexactinellids (>3.5 m) in deep-water reefs (Wagner and Kelley 2016). Interestingly, these same patterns are not observed in osculum size. While osculum size was smaller for archaeocyaths, the difference between these and modern organisms was not nearly as large, and there was no difference in variance. While an exhaustive search

was not performed, selected modern demosponges had an average of 9.9 ± 15.1 ($N = 4$) oscula per sponge, with several more containing more than a hundred. By comparison, nearly all archaeocyaths contained a single osculum. Increasing osculum size can reduce pumping efficiency; therefore, it may be more energetically favorable to produce many smaller oscula rather than expanding a single large one when expanding body size (Palumbi 1986).

Comparing archaeocyaths to lithistid sponges, we find that while a greater proportion of lithistid sponges surveyed as part of this study were within the body-size range of archaeocyaths, they were on average larger (Fig. 3, Table 1). This pattern remained even after separating fossil and modern lithistid sponges, which themselves showed a change in size through time, with the average fossil lithistid sponge within the range of archaeocyathan body size, but significantly larger overall.

Discrete characteristics also show that archaeocyaths had a limited number of morphologies. Modern demosponges are most commonly encrusting or massive, and lithistid sponges are most often conical (Fig. 4A). While some archaeocyaths—for example, *Retilamina*, domal shape and possible encrusting habit; order Kazachstanicyathida and suborder Dictyofavina, stromatoporoid-grade shape and massive habit (Debrenne et al. 1991)—possess unique gross morphologies, these genera make up <3% of archaeocyaths. Otherwise, archaeocyaths usually have a simple erect habit. Furthermore, archaeocyaths rarely possess specialized elaborations that in other sponges can increase surface exposure and hydrodynamic properties (Church 2017). Branching morphologies are most common in modular archaeocyaths, and even these are often weakly integrated. A previous study by Wood et al. (1992) found that 94.7% of archaeocyathan species were either solitary or weakly integrated ($N = 508$). This could lead to greater susceptibility to changes in environmental conditions or storms that could fragment poorly supported branching organisms (Wood et al. 1992). We find that archaeocyaths have smaller average body sizes, lower size variability, and lower diversity of gross morphology compared
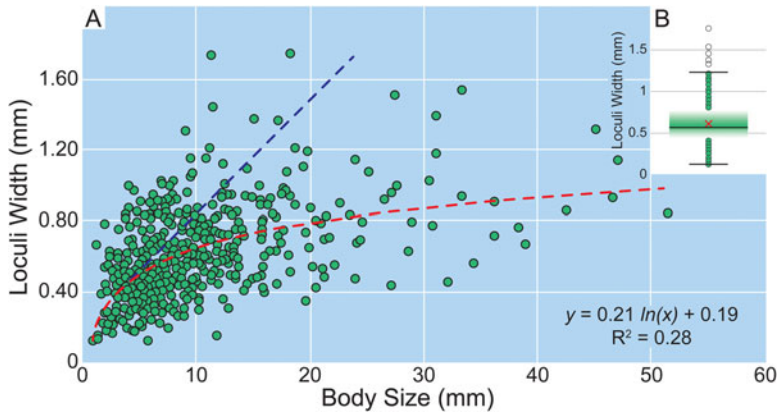
FIGURE 6. Loculus size distribution of archaeocyaths. A, Body size to loculus width relationship with logarithmic trend line shown in red. Purple line shows hypothetical continuation of loculus sizes if a linear trend of increasing width with increasing body size were occurring. Readers are directed to the online version of this article for color figures. B, Box-and-whisker plot of loculus widths; "X" denotes arithmetic mean. Raw data available in the Supplementary Materials.

with other types of sponges, resulting in overall restricted morphospace occupancy.

This study only focused on two endpoints of the Phanerozoic to assess changes in reef-building sponge morphology (Fig. 5F). A more thorough study of the Phanerozoic would be required to assess when this change occurred, but it may most likely be tied to when archaeocyaths ceased being the primary metazoan reef-building organisms (see Lee and Riding [2018] for a study on size changes in reef builders). Spiculate sponges within the order Protomonaxonida were already equal to or larger than archaeocyaths, with diameters between 5 and 40 mm (Xiao et al. 2005; Botting and Peel 2016), but were confined to low-energy environments until the Ordovician (Carrera and Botting 2008). During the Miaolingian, explanate lithistid sponges formed in reefs measured between 7 and 23 mm (Kruse and Reitner 2014: Figs. 6A, 14). But larger lithistid sponges grew to ~2 cm wide during the Miaolingian of China (Lee et al. 2016) and even larger in Iran and the western United States by the late Cambrian (Shapiro and Rigby 2004; Kruse and Zhuravlev 2008; Lee and Riding 2018). Pulchrilaminids and stromatoporoids (Early and Middle Ordovician, respectively) later occurred in reefs, and they too were larger than early Cambrian archaeocyaths (Li et al. 2016; Hong et al. 2017). Thus, it seems that archaeocyaths had a limited size range and morphological disparity, which

was unique for reef-building sponges in the early Paleozoic.

Why Were Archaeocyaths So Small?

The size of loculi within the intervallum does not appear to scale linearly with body size (Fig. 6A). Rather, loculus width is maintained by the insertion of new septa once the loculus width attains a certain size (McKee 1963), with a maximum loculus width at approximately 1.25 mm (Fig. 6B). At small body sizes (<10 mm) there is a stronger correlation ($r = 0.35$) compared with larger (>10 mm) body sizes ($r = 0.27$). Flume-tank experiments with archaeocyathan models have shown that septa increase water entrainment and support unidirectional flow through the central cavity (Savarese 1992). Therefore, it is possible that larger loculus widths would reduce the efficiency of flow patterns and hinder filter feeding (Fig. 5G,H).

Archaeocyaths could not grow to larger sizes, as it would have been too energetically expensive to produce additional biomineralized septa to help direct fluid flow. This challenge would have been further exacerbated by the low calcite saturation state of the late-early Cambrian oceans (Pruss et al. 2010; Knoll and Fischer 2011; Riding et al. 2019), which negatively impacts calcification of reef builders (Cohen and Holcomb 2009), as well as changing seawater chemistry from aragonite to calcite seas (Lowenstein et al. 2001; Porter 2010)

that has been correlated with reef-builder extinctions (Zhuravlev and Wood 2009; Kiessling and Simpson 2010). Furthermore, planktonic food sources may have been lower until the late Cambrian, limiting suspension-feeder food supply (Servais et al. 2016).

The hypothesized reliance on passive entrainment and the unique double-walled calcareous structure, which occupies over 20% of the archaeocyathan body, may represent a form of self-limiting modularity within the archaeocyathan body plan (Table 1). Modern experiments on glass sponges show that passive entrainment is critical for sponges, but is probably only plausible in sponges with thin walls and large oscula (Leys et al. 2011).

This same evolutionary trade-off can be seen in modern examples of calcareous demosponges, though suspension feeding is aided by active pumping with choanocytes as well as passive entrainment. The modern sponge *Vaceletia crypta* has reliably been placed within the order Demospongiae based on molecular systematics (Wörheide 2008), despite possessing an aspiculate, aragonite skeleton with stacked chambers. Superficial similarities to Archaeocyatha have led some to suggest an ancestral relationship between the two (Pickett 1985); however, the earliest fossil record of *Vaceletia* is from the Triassic and would imply a long fossil record gap. Even if *Vaceletia* is not a direct descendant, a comparison of its morphology can still be useful to understanding the archaeocyathan body plan. *Vaceletia* displays a gross morphology with a single osculum and size (mm to cm) similar to many archaeocyaths (Wörheide and Reitner 1996; Germer et al. 2015).

Extinct sponge taxa also show these patterns. For instance, Triassic examples of chambered "sphinctozoan" sponges also show a convergent robust calcareous skeleton and rarely measure above 130 mm, with most being far smaller (see Senowbari-Daryan and Stanley 1992; Senowbari-Daryan and Zamparelli 2003). In contrast, hypercalcifying labechiid stromatoporoid sponges also lacked spicules, but could achieve large body sizes up to 15 cm across (Stern et al. 1999; Hong et al. 2017). Stromatoporoid sponges do not contain the same double-walled structure and instead have more densely packed, but thin, laminae and pillars (Wolniewicz 2009) and astrorhizal canals that provide a more distributed and energetically efficient fluid-entrainment system (Boyajian and LaBarbera 1987; LaBarbera and Boyajian 1991; LaBarbera 1993). Additionally, the Ordovician hypercalcifying sponge *Calathium*, which may have close affinities to archaeocyaths, has been measured at sizes of 300 mm in length and 90 mm in diameter (Li et al. 2015). *Calathium* is superficially similar to archaeocyaths, as both have calcified inner and outer walls. However, *Calathium* walls are connected by rods as opposed to septa, which may alter the physiological demands of building such structures.

Modern spiculate sponges do not produce thick skeletons and can therefore devote more energy to body expansion and more diverse gross morphologies. It may be that spicules present a less energy-intensive method of extending the sponge body off the seafloor while still maintaining a flexible body plan to adapt to local conditions (Uriz et al. 2003; Nickel et al. 2006), a condition not afforded by rigid calcareous skeletons. In short, sponges with both a chambered modular structure and calcareous skeletons tend to be smaller than organisms that lack one or the other. The small body size and simple morphology of both archaeocyaths and *Vaceletia* are consistent with our interpretation that the trade-off of building a calcareous skeleton with a unique double-walled (and/or chambered) structure is limited body size and morphological disparity.

Conclusions

We provide evidence that archaeocyaths from the early Cambrian of Laurentia were relatively restricted in both body size and gross morphological disparity. In comparison with archaeocyaths, modern demosponges and lithistid sponges are as much as an order of magnitude greater in body size and body-size variability. Furthermore, both groups are well distributed across several gross morphological categories compared with a sparser distribution for archaeocyaths. In a larger context, we find that morphospace occupancy of early Cambrian reef-building sponges was reduced

compared with other sponge taxa. This suggests that morphospace occupancy for reef builders expanded, potentially sometime during the early Paleozoic, and may have contributed to increases in biodiversity in macroscopic reef builders during the Ordovician (Cordie et al. 2019). Their limited morphospace occupancy suggests that archaeocyaths of Laurentia did not adapt to a variety of environmental conditions. The restricted morphological disparity of archaeocyaths may have played a role in their ability to create additional niche space and resistance to habitat change (Wulff 2006; Kerry and Bellwood 2012). By investigating the morphospace of early Cambrian reef builders, we further support the transitional nature of the Cambrian as a period of establishment of the basic ecological properties common in ecosystems today, but with more restricted diversity.

Acknowledgments

Literature Cited

Balsam, W. L., and S. Vogel. 1973. Water movement in archaeocyathids: evidence and implications of passive flow models. Journal of Paleontology 47:979–984.

Barthel, D., and A. Brandt. 1995. *Caecognathia robusta* (G.O. Sars, 1879) (Crustacea, Isopoda) in *Geodia mesotriaena* (Hentschel, 1929) (Demospongiae, Choristidae) at 75° N off NE Greenland. Sarsia 80:223–228.

Bell, J. J., and D. K. A. Barnes. 2000. The influences of bathymetry and flow regime upon the morphology of sublittoral sponge communities. Journal of Marine Biological Association of the United Kingdom 80:707–718.

——. 2001. Sponge morphological diversity: a qualitative predictor of species diversity? Aquatic Conservation: Marine and Freshwater Ecosystems 11:109–121.

Bell, J. J., D. K. A. Barnes, and J. R. Turner. 2002. The importance of micro and macro morphological variation in the adaptation of a sublittoral demosponge to current extremes. Marine Biology 140:75–81.

Bellwood, D. R., C. H. R. Goatley, S. J. Brandl, and O. Bellwood. 2014. Fifty million years of herbivory on coral reefs: fossils, fish and functional innovations. Proceedings of the Royal Society of London B 281:20133046.

Botting, J. P., and J. S. Peel. 2016. Early Cambrian sponges of the Sirius Passet Biota, North Greenland. Papers in Palaeontology 2:463–487.

Boury-Esnault, N., and K. Rützler. 1997. Thesaurus of sponge morphology. Smithsonian contributions to zoology 596. Smithsonian Institution, Washington, D.C.

Boyajian, G. E., and M. LaBarbera. 1987. Biomechanical analysis of passive flow stromatoporoids—morphologic, paleoecologic, and systematic implications. Lethaia 20:223–229.

Briggs, D. E. G., R. A. Fortey, and M. A. Willis. 1992. Morphological disparity in the Cambrian. Science 256:1670–1673.

Carrera, M. G., and J. P. Botting. 2008. Evolutionary history of Cambrian spiculate sponges: implications for the Cambrian Evolutionary Fauna. Palaios 23:124–138.

Church, S. B. 2017. Efficient ornamentation in Ordovician anthaspidellid sponges. Paleontological Contributions 18:1–8.

Cohen, A. L., and M. Holcomb. 2009. Why corals care about ocean acidification: uncovering the mechanism. Oceanography 22:118–127.

Cohen, J. 1992. A power primer. Psychological Bulletin 112:155–159.

Cordie, D. R., S. Q. Dornbos, P. J. Marenco, T. Oji, and S. Gonchigdorf. 2019. Depauperate skeletonized reef-dwelling fauna of the early Cambrian: insights from archaeocyathan reef ecosystems of western Mongolia. Palaeogeography, Palaeoclimatology, Palaeoecology 514:206–221.

Debrenne, F., and A. Zhuravlev. 1992. Irregular archaeocyaths. CNRS Editions, Paris.

——. 1994. Archaeocyathan affinities: how deep can we go into the systematic affiliation of an extinct group? Pp. 3–12 in R. W. M. van Soest, T. M. G. van Kempen, and J. C. Braekman, eds. Sponges in time and space. Balkema, Rotterdam.

Debrenne, F., A. Rozanov, and A. Zhuravlev. 1990. Regular archaeocyaths. CNRS Editions, Paris.

Debrenne, F., P. D. Kruse, and Z. Sengui. 1991. An Asian compound archaeocyath. Alcheringa 15:285–291.

Debrenne, F., A. Y. Zhuravlev, and P. D. Kruse. 2015. General features of the Archaeocyatha. Pp. 845–1084 in F. Debrenne, W. D. Hartman, S. Kershaw, P. D. Kruse, H. Nestor, J. K. Rigby, Sr., B. Senowbari-Daryan, C. W. Stern, C. W. Stock, J. Vacelet, B. D. Webby, R. R. West, P. Willenz, R. A. Wood, and A. Y. Zhuravlev. Porifera (revised), vol. 5, Hypercalcified Porifera. Part E of P. A. Selden, ed. Treatise on invertebrate paleontology. Geological Society of America, New York, and University of Kansas, Lawrence.

Erwin, D. H. 2007. Disparity: morphological pattern and development context. Palaeontology 50:57–73.

——. 2008. Macroevolution of ecosystem engineering, niche construction and diversity. Trends in Ecology and Evolution 23:304–310.

Foote, M. 1992. Paleozoic record of morphological diversity in blastozoan echinoderms. Proceedings of the National Academy of Sciences USA 89:7325–7329.

Germer, J., K. Mann, G. Wörheide, and D. J. Jackson. 2015. The skeleton forming proteome of an early branching metazoan: a molecular survey of the biomineralization components employed by the coralline sponge *Vacelatia* sp. PLoS ONE 10:e0140100.

Ghiold, J., G. A. Rountree, and S. H. Smith. 1994. Common sponges of the Cayman Islands. The Cayman Islands. Pp. 131–138 in M. A. Brunt and J. E. Davies, eds. The Cayman Islands: natural history and biogeography. Kluwer Academic, Dordrecht, Netherlands.

Gili, C., and J. Marinell. 1994. Relationship between species longevity and larval ecology in nassariid gastropods. Lethaia 27:291–299.

Gould, S. J. 1991. The disparity of the Burgess Shale arthropod fauna and the limits of cladistic analysis: why we must strive to quantify morphospace. Paleobiology 17:411–423.

Gray, E. L., C. J. Burwell, and A. M. Baker. 2016. Benefits of being a generalist carnivore when threatened by climate change: the comparative dietary ecology of two sympatric semelparous marsupials, including a new endangered species (*Antechinus arktos*). Australian Journal of Zoology 64:249–261.

Hageman, S. J., and F. K. McKinney. 2010. Discrimination of fenestrate bryozoan genera in morphospace. Palaeontologia Electronica 13:1–43.

Hellberg, M. E., D. P. Balch, and K. Roy. 2001. Climate-driven range expansion and morphological evolution in a marine gastropod. Science 292:1707–1710.

Hicks, M. 2006. A new genus of early Cambrian coral in Esmeralda county, southwestern Nevada. Journal of Paleontology 80:609–615.

Hill, D. 1964. The phylum Archaeocyatha. Biological Review 39:232–258.

Hong, J., S.-J. Choh, J. Park, and D.-J. Lee. 2017. Construction of the earliest stromatoporoids framework: labechiid reefs from the Middle Ordovician of Korea. Palaeogeography, Palaeoclimatology, Palaeoecology 470:54–62.

Hooper, J. N. A., and R. W. M. Van Soest, eds. 2002. Systema Porifera: a guide to the classification of sponges, Vol. 1. Kluwer Academic/Plenum, New York.

Huang, S., K. Roy, and D. Jablonski. 2014. Origins, bottlenecks, and present-day diversity: patterns of morphospace occupation in marine bivalves. Evolution 69:735–746.

Jablonski, D., and G. Hunt. 2006. Larval ecology, geographic range, and species survivorship in Cretaceous mollusks: organismic versus species-level explanations. American Naturalist 168:556–564.

Kammer, T. W., T. K. Baumiller, and W. I. Ausich. 1997. Species longevity as a function of niche breadth: evidence from fossil crinoids. Geology 25:219–222.

——. 1998. Evolutionary significance of differential species longevity in Osagean–Meramecian (Mississippian) crinoid clades. Paleobiology 24:155–176.

Kerner, A., F. Debrenne, and R. Vignes-Lebbe. 2011. Cambrian archaeocyath metazoans: revisions of morphological characters and standardization of genus descriptions to establish an online identification tool. *In* V. Smith and I. Penev, eds. e-Infrastructure for data publishing in biodiversity science. ZooKeys 150:381–395.

Kerry, J. T., and D. R. Bellwood. 2012. The effect of coral morphology on shelter selection by coral reef fishes. Coral Reefs 31:415–424.

Kiessling, W., and C. Simpson. 2010. On the potential for ocean acidification to be a general cause of ancient reef crisis. Global Change Biology 17:56–67.

Knoll, A. H., and W. W. Fischer. 2011. Skeletons and ocean chemistry: the long view. Pp. 67–82 *in* J.-P. Gattuso and L. Hansson. eds. Ocean acidification. Oxford University Press, Oxford.

Kruse, P. D., and J. R. Reitner. 2014. Northern Australian microbial-metazoan reefs after the mid-Cambrian mass extinction. Memoirs of the Association of Australian Palaeontologists 45:31–53.

Kruse, P. D., and A. Y. Zhuravlev. 2008. Middle-late Cambrian *Rankenella-Girvanella* reefs of the Mila Formation, northern Iran. Canadian Journal of Earth Science 45:619–639.

Kruse, P. D., A. Gandin, F. Debrenne, and R. Wood. 1996. Early Cambrian bioconstructions in the Zavkhan Basin of western Mongolia. Geological Magazine 133:429–444.

LaBarbera, M. 1993. The astrorhizae of fossil stromatoporoids closely approximate an energically optimal fluid transport system. Experientia 49:539–541.

LaBarbera, M., and G. E. Boyajian. 1991. The function of astrorhizae in stromatoporoids: quantitative tests. Paleobiology 17:121–132.

Lee, J.-H., J. Hong, S.-J. Choh, D.-J. Lee, J. Woo, and R. Riding. 2016. Early recovery of sponge framework reefs after Cambrian archaeocyath extinction: Zhangxia Formation (early Cambrian Series 3), Shandong, North China. Palaeogeography, Palaeoclimatology, Palaeoecology 457:269–276.

Lee, J.-H., and R. Riding. 2018. Marine oxygenation, lithistid sponges, and the early history of Paleozoic skeletal reefs. Earth-Science Reviews 181:98–121.

Lefebvre, B., G. J. Eble, N. Navarro, and B. David. 2006. Diversification of atypical Paleozoic echinoderms: a quantitative survey of patterns of stylophoran disparity, diversity, and geography. Paleobiology 32:483–510.

Leys, S. P., G. Yahel, M. A. Reibenbach, V. Tunnicliffe, U. Shavit, and H. M. Reiswig. 2011. The sponge pump: the role of current induced flow in the design of the sponge body plan. PLoS ONE 6:e27787.

Li, Q., Y. Li, J. Wang, and W. Kiessling. 2015. Early Ordovician lithistid sponge-*Calathium* reefs on the Yangtze Platform and their paleoceanographic implications. Palaeogeography, Palaeoclimatology, Palaeoecology 425:84–96.

Li, Q., Y. Li, and W. Kiessling. 2016. The oldest labechiid stromatoporoids from intraskeletal crypts in lithistid sponge-*Calathium* reefs. Lethaia 50:140–148.

Liu, B., J. K. Rigby, and Z. Zhu. 2003. Middle Ordovician lithistid sponges from the Bachu-Kalpin Area, Xinjiang, northwestern China. Journal of Paleontology 77:430–441.

Löfgren, A. S., R. E. Plotnick, and P. J. Wagner. 2003. Morphological diversity of Carboniferous arthropods and insights on disparity patterns through the Phanerozoic. Paleobiology 29:349–368.

Losos, J. B. 2010. Adaptive radiation, ecological opportunity, and evolutionary determinism. American Naturalist 175:623–639.

Lowenstein, T. K., M. N. Timofeeff, S. T. Brennan, L. A. Hardie, and R. V. Demicco. 2001. Oscillations in Phanerozoic seawater chemistry: evidence from fluid inclusions. Science 294:1086–1088.

McCormack, J. E., and T. B. Smith. 2008. Niche expansion leads to small-scale adaptive divergence along an elevation gradient in a medium-sized passerine bird. Proceedings of the Royal Society of London B 275:2155–2164.

McKee, E. H. 1963. Ontogenetic stages of the archaeocyathid *Ethmophyllum whitneyi* Meek. Journal of Paleontology 37:287–293.

McMurray, S. E., J. E. Blum, and J. R. Pawlik. 2008. Redwood of the reef: growth and age of the giant barrel sponge *Xestospongia muta* in the Florida Keys. Marine Biology 155:159–171.

Mitteroecker, P., and S. M. Huttegger. 2009. The concept of morphospaces in evolutionary and developmental biology: mathematics and metaphors. Biological Theory 4:54–67.

Nickel, M., E. Bullinger, and F. Beckmann. 2006. Functional morphology of *Tethya* species (Porifera): 2. Three-dimensional morphometrics on spicules and skeletal superstructures of *T. minuta*. Zoomorphology 125:225–239.

Palumbi, S. R. 1984. Tactics of acclimation: morphological changes of sponges in an unpredictable environment. Science 225:1478–1480.

——. 1986. How body plans limit acclimation: responses of a demosponge to wave force. Ecology 67:208–214.

Pickett, J. 1985. *Vaceletia*, the living archaeocyathid. New Zealand Geological Survey Record 9:77.

Porter, S. M. 2010. Calcite and aragonite seas and the *de novo* acquisition of carbonate skeletons. Geobiology 8:256–277.

Pruss, S. B., S. Finnegan, W. W. Fischer, and A. H. Knoll. 2010. Carbonates in skeleton-poor seas: new insights from Cambrian and Ordovician strata of Laurentia. Palaios 25:73–84.

Raia, P., F. Carotenuto, A. Mondanaro, S. Castiglione, F. Passaro, F. Saggese, M. Melchionna, C. Serio, L. Alessio, D. Silvestro, and M. Fortelius. 2016. Progress to extinction: increased specialization causes the demise of animal clades. Scientific Reports 6:30965.

Raup, D. M. 1966. Geometric analysis of shell coiling: general problems. Journal of Paleontology 40:1178–1190.

Reitner, J., N. Langsford, and P. D. Kruse. 2017. An unusual ferruginous-calcitic *Frutexites* microbialite community from the lower Cambrian of the Flinders Ranges, South Australia. Paläontologische Zeitschrift 91:1–3.

Riding, R., L. Liang, J.-H. Lee, and A. Virgone. 2019. Influence of dissolved oxygen on secular patterns of marine microbial carbonate abundance during the past 490 Myr. Palaeogeography, Palaeoclimatology, Palaeoecology 514:135–143.

Ritterbush, K. A., and D. J. Bottjer. 2012. Westermann morphospace displays ammonoid shell shape and hypothetical paleoecology. Paleobiology 38:424–446.

Rowland, S. M. 2001. Archaeocyaths—a history of phylogenetic interpretation. Journal of Paleontology 75:1065–1078.

Savarese, M. 1992. Functional analysis of archaeocyath skeletal morphology and its paleobiological implications. Paleobiology 18:464–480.

——. 1995. Functional significance of regular archaeocyath central cavity diameter: a biomechanical and paleoecological test. Paleobiology 21:356–378.

Savarese, M., and P. W. Signor. 1989. New archaeocyathan occurrences in the upper Harkless Formation (Lower Cambrian of western Nevada). Journal of Paleontology 63:539–549.

Schuster, A., D. Erpenbeck, A. Pisera, J. Hooper, M. Bryce, J. Fromont, and G. Wörteide. 2015. Deceptive desmas: molecular phylogenetics suggests a new classification and uncovers convergent evolution of lithistid demosponges. PLoS ONE 10:e116038.

Senowbari-Daryan, B., and G. D. Stanley. 1992. Late Triassic thalamid sponges from Nevada. Journal of Paleontology 66:183–193.

Senowbari-Daryan, B. and V. Zamparelli. 2003. Upper Triassic (Norian–Rhaetian) new thalamid sponges from northern Calabria (southern Italy). Studia Universitatis Babeş–Bolyai, Geologia 48:113–124.

Servias, T., V. Perrier, T. Danelian, C. Klug, R. Martin, A. Munnecke, H. Nowak, A. Nützel, T. R. A. Vandenbroucke, M. Williams, and C. M. Ø. Rasmussen. 2016. The onset of the "Ordovician Plankton Revolution" in the late Cambrian. Palaeogeography, Palaeoclimatology, Palaeoecology 458:12–28.

Shapiro, R. S., and J. K. Rigby. 2004. First occurrence of an in situ anthaspidellid sponge in a dendrolite mound (upper Cambrian; Great Basin, USA). Journal of Paleontology 78:645–650.

Shen, B., L. Dong, S. Xiao, and M. Kowalewski. 2008. The Avalon explosion: evolution of Ediacara morphospace. Science 319:81–84.

Stanley, S. M. 1986. Population size, extinction, and speciation: the fission effect in Neogene Bivalvia. Paleobiology 12:89–110.

Stern, C. W., B. D. Webby, H. Nestor, and C. W. Stock. 1999. Revised classification and terminology of Palaeozoic stromatoporoids. Acta Palaeontologica Polonica 44:1–70.

Uriz, M-J., X. Turon, M. A. Becerro, and G. Agell. 2003. Siliceous spicules and skeletal frameworks in sponges: origin, diversity, ultrastructure patterns, and biological functions. Microscopy Research and Technique 62:279–299.

Wagner, D., and C. D. Kelley. 2016. The largest sponge in the world? Marine Biodiversity 47:367–368.

Watkins, R. 2000. Corallite size and spacing as an aspect of niche–partitioning in tabulate corals of Silurian reefs, Racine Formation, North America. Lethaia 33:55–63.

Webby, B. D. 1979. The oldest Ordovician stromatoporoids from Australia. Alcheringa 3:237–251.

Willis, M. A. 1998. Cambrian and recent disparity: the picture from priapulids. Paleobiology 24:177–199.

Wilson, S. K., S. C. Burgess, A. J. Cheal, M. Emslie, R. Fisher, I. Miller, N. V. C. Polunin, and H. P. A. Sweatman. 2007. Habitat utilization by coral reef fish: implications for specialists vs. generalists in a changing environment. Journal of Animal Ecology 77:220–228.

Wolniewicz, P. 2009. Late Framennian stromatoporoids from Dębnik Anticline, Southern Poland. Acta Palaeontologica Polonica 54:337–350.

Wood, R. 1995. The changing biology of reef-building. Palaios 10:517–529.

Wood, R., A. Y. Zhuravlev, and F. Debrenne. 1992. Functional biology and ecology of archaeocyatha. Palaios 7:131–156.

Wörheide, G. 2008. A hypercalcified sponge with soft relatives: *Vaceletia* is a keratose demosponge. Molecular Phylogenetics and Evolution 47:433–438.

Wörheide, G., and J. Reitner. 1996. "Living fossil" sphinctozoan coralline sponge colonies in shallow water caves of the Osprey Reef (Coral Sea) and the Astrolabe Reefs (Fiji Islands). Pp. 145–148 *in* J. Reitner, F. Neuweiler, and F. Gunkel. eds. Göttinger Arbeiten zur Geologie und Paläeontologie. University of Goettingen, Goettingen, Germany.

Wulff, J. L. 2006. Resistance vs recovery: morphological strategies of coral reef sponges. Functional Ecology 20:699–708.

Xiao, S., J. Hu, X. Yuan, R. L. Parsley, and R. Cao. 2005. Articulated sponges form the lower Cambrian Hetang Formation in southern Anhui, South China: their age and implications for the early evolution of sponges. Palaeogeography, Palaeoclimatology, Palaeoecology 220:89–117.

Yang, J., J. Ortega-Hernández, S. Gerber, N. J. Butterfield, J.-B. Hou, T. Lan, and X.-G. Zhang. 2015. A superarmored lobopodian from the Cambrian of China and early disparity in the evolution of Onychophora. Proceedings of the National Academy of Sciences USA 114:8678–8683.

Zhuravlev, A. Y., and R. A. Wood. 2009. Controls on carbonate skeletal mineralogy: global CO_2 evolution and mass extinctions. Geology 37:1123–1126.